# Retinal HDR Images: The Effects of Intraocular Glare and Object Size

**John J. McCann[1] and A. Rizzi[2]**

**[1]*McCann Imaging, Belmont, MA 02478, USA***

**[2]*Dipartimento di Tecnologie dell'Informazione,
Università degli Studi di Milano, 26013 Crema (CR), Italy***

# Retinal HDR Images: The Effects of Intraocular Glare and Object Size

## Abstract

Starting from measured *scene* luminances, we calculated the *retinal* luminance images of High Dynamic Range (HDR) test targets. These test displays contain 40 gray squares with a 50% average surround. In order to approximate a natural scene the 50% surround area was made up of half-white and half-black squares of different sizes. In this way, the spatial-frequency distribution approximates a 1/f function of energy vs. spatial frequency. We compared images with 2.7 and 5.4 optical density ranges. Although the target ranges were very different, the retinal luminances are very similar. Intraocular glare restricts the range of the retinal image. Further, uniform, equiluminant target patches are spatially transformed to different gradients with unequal retinal luminance. The usable dynamic range of the display correlates with the range of retinal luminances. The appearance of whites and blacks in the display correlates better with the target luminances, than with retinal luminances. Since human spatial image processing increases apparent contrast with larger areas of white in the surround, spatial vision counteracts glare. The spatial contrast mechanism is much more powerful when compared with retinal luminance, than with target luminance.

## 1. Introduction

At times, research on human vision describes detailed information about the stimulus using radiometric, or photometric, measurements of the scene, or of the test target. Studies analyzing human image processing need to consider the light distribution of the image falling on the retina after intraocular scatter.

High Dynamic Range (HDR) imaging is a good example. HDR images capture and display a greater range of information than conventional images[1,2]. However, scene-dependent scatter in cameras, and in the human eye, control the ranges of information, and appearances.[2] We studied the effects of intraocular scatter and the size of image elements with calculated retinal images. We used van den Berg's CIE scatter standard[3,4,5] to calculate the image on the retina. We found large changes in spatial distribution of retinal luminances compared to target luminances. The retinal luminances changed dramatically with change in the size of target elements.

## 2. Design of Target

We want to measure how veiling glare affects tone scale functions that relate display luminance to appearance in HDR images. To start, we can set aside all the complexities introduced by gradients in illumination. We will just study patches of light that are uniform in the target.[6]

We used a surround that is, on average, equal to the middle of the dynamic range (50% max and 50% min luminance).[7] Further, these surround elements are made up of different size min and max blocks, spatially unevenly distributed, so that the image has energy over a wide range of spatial frequencies. It avoids the problem that simultaneous contrast depends on the relative size of the white areas and the test patch.[8] Plots of the radial spatial frequency distribution vs. frequency approximate the 1/f distribution[9] found in natural images.

### 2.1 Targets Layout

Figures 1 & 2 show the layout of the min/max test target. The display subtended 15.5 by 19.1 degrees. It was divided into 20 squares, 3.4 degrees on a side. Two 0.8 degree gray patches are within each square along with various sizes of max and min blocks. The two gray square length subtends an angle approximately the diameter of the fovea. The smallest block (surrounding the gray patches) subtends 1.6 minutes of arc and is clearly visible

to observers.  Additional blocks 2x, 4x, 8x, 16x, 32x, 64x are used in the surround for each gray pair.
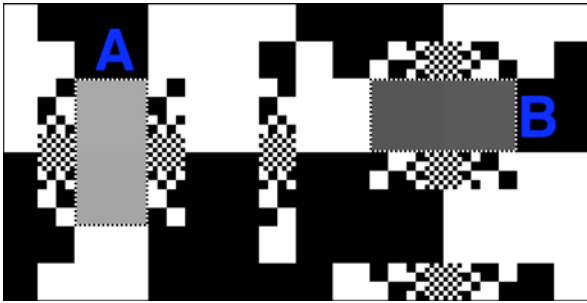


Figure 1 shows a magnified view of two of twenty gray pairs of luminance patches.  The left half (square A) has the same layout as the right (square B), rotated 90° clockwise.  The gray areas in A have slightly different luminances, top and bottom. The gray areas in B have different luminances, left and right.  The square surrounding areas are identical except for rotation.  For each size there are equal numbers of min and max blocks.
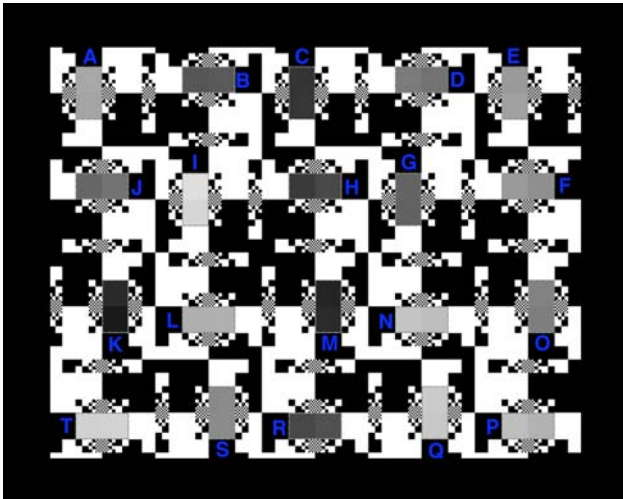


Figure 2 shows all twenty gray pairs of luminance patches.  All gray pairs are close in luminance, but some edge ratios are larger than others.

## 2.2 Single- and Double-Density Targets

Figure 2 shows the 4 by 5 in. film transparency (Single Density) test target. We calculated the array of retinal luminances from the array of measured uniform target luminances. The Double-Density target was the aligned superposition of two identical (Single-Density) films.

Two transparencies double the optical densities (OD). [Optical Density = log10 (1/transmittance) ]  The whites in each transparency have an optical density (O.D.) of 0.19; the blacks have an O.D. of 2.89.  The Double Density images have a min of 0.38 and a max of 5.78 O.D (See Table 1). Both transparency configurations are backlit by 4 diffused neon bulbs.

| Target | Max cd/m² | Min cd/m² | Range:1 | %Average cd/m² | O.D. Min | O.D. Max | O.D. Range |
|---|---|---|---|---|---|---|---|
| Single Contrast | 684 | 1.36 | 501 | 50.01% | 0.19 | 2.89 | 2.70 |
| Double Contrast | 441 | 0.0018 | 251,189 | 50.00% | 0.38 | 5.78 | 5.40 |

Table 1 list the luminances and optical densities of the min and max areas in Single- and Double-Density (Contrast) displays.

Veiling glare for Human Visual System (HVS) is a property of the luminance of each image pixel and the glare spread function (GSF) of the human optical system. Surrounds made up of half-max and half-min luminances have nearly the same glare properties for Single- and Double-Density test targets.  The average luminance of the Single-Density target is 50.10% of the maximum luminance, from a display with a range of ~500:1.  The average luminance of the Double-Density target is 50.00% of its maximum luminance, from a display with a range of ~250,000:1.  The effect of glare on the luminances of the gray test areas will be very nearly the same, despite the fact that the dynamic range has changed from 500:1 to 250,000:1.  In other words, the black areas (min luminances) in both Single- and Double-Density targets are so low they make only trivial contributions to glare.  The white (max luminances) in both targets are almost equal and generate virtually all the glare.  The layouts of both targets are constant. The physical contributions of glare are very nearly constant.  By comparing the calculated retinal luminances of appearance of these Single- and Double-Density targets, we can measure the effects of constant glare on very different dynamic-range displays.
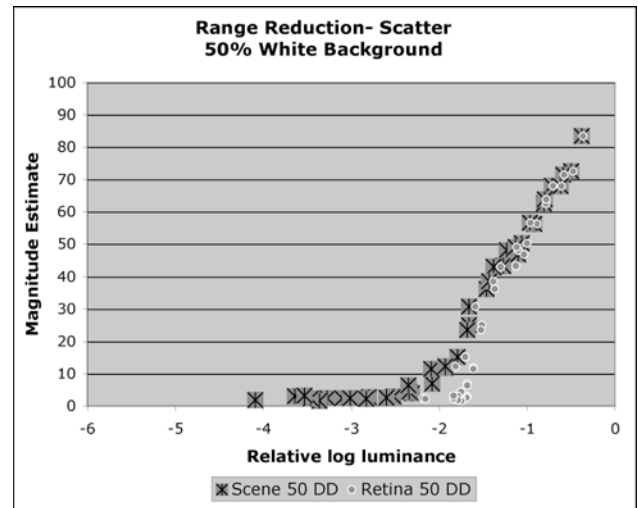


Figure 3 plots the relative target (crosses) and retinal (dots) luminances vs. observed magnitude estimates of appearance [Magnitude estimate 100 = white; 1=black].

Figure 3 plots the average magnitude estimates (DD) from five trials with five observers less than 30 years old. Observers can discriminate gray appearances over a range

of target luminances of 2.8 log units, the range of stimuli. Calculated retinal luminances (described below) show the reduced range due to intraocular scatter.

# 3. Calculated Retinal Luminance

There are three steps in determining the luminances falling on the retina. First, we need to measure the luminance at each pixel in the scene. Second, we need to determine which glare point spread function best represents the one of human vision. Third, we need to create an efficient algorithm that can read the entire scene array and, taking into account viewing distance and other parameters, transform scene luminances to retinal luminances.

## 3.1 Input luminance array

The first step in the calculation is to read the digital array and use the appropriate calibration LUT to convert digit to target OD, and then to measured luminance (cd/m$^2$). The lightbox has a luminance of 1059 cd/m$^2$. We used all the optical density measurements of white, black, gray calibration squares on the side of both transparencies to create a LUT for each target. This program reads a digit from the file sent to the film recorder, looks up the measured optical density and reduces the light box luminance by the corresponding % transmission value. The program reads the 0-255 value in the digital array and replaces it with the floating point luminance value accurate over 6 log units. This accuracy is assured by the densitometer measurements of each separate single transparency against calibrated standard samples.

## 3.2 van den Berg's CIE scatter standard

1939 CIE meeting reported an empirical description of veiling glare estimated proportional to $1/\theta^2$, J. Vos and T. van den Berg collected a series of measurements and wrote a more recent CIE report[3], dated 1999, in which a whole set of formulas are proposed according to the desired degree of precision and other parameters like the age of the observer and the type of his pigment.

We decided to report in this paper results from the formula referred as number [8] in the report[3] since it is the most complete. See Figure 4. This formula measures the equivalent veiling glare in relation to the energy of relative illuminance and is defined as $\left[ sr^{-1} \right]$.

The formula is the following:

$$L_{eq}/E_{gl} = \left[1 - 0.08 \cdot (A/70)^4\right] \cdot \left[\frac{9.2 \cdot 10^6}{\left[1 + (\theta/0.0046)^2\right]^{1.5}} + \frac{1.5 \cdot 10^5}{\left[1 + (\theta/0.045)^2\right]^{1.5}}\right] +$$

$$+ \left[1 - 1.6 \cdot (A/70)^4\right] \cdot \left\{\left[\frac{400}{1 + (\theta/0.1)^2} + 3 \cdot 10^{-8} \cdot \theta^2\right] + p \cdot \left[\frac{1300}{\left[1 + (\theta/0.1)^2\right]^{1.5}} + \frac{0.8}{\left[1 + (\theta/0.045)^2\right]^{0.5}}\right]\right\} + 2.5 \cdot 10^{-3} \cdot p$$

where $\theta$ is the viewing angle from the point from which the light is spread causing the veiling glare, $A$ is the age of the observer and $p$ is his/her iris pigmentation. This formula measures the equivalent veiling glare in relation to the energy of relative illuminance and is defined as $\left[ sr^{-1} \right]$. Pigmentation types give the origin of correction parameters that ranges from 0 to 1.21. In the test we used an age of 25 and brown Caucasian pigment.

## 3.3 Applying the filter

We used Matlab$^©$ to compute the Glare Spread Function (GSF) from the CIE formula reported above and to convolve it with the calibrated input image converted into luminance values.
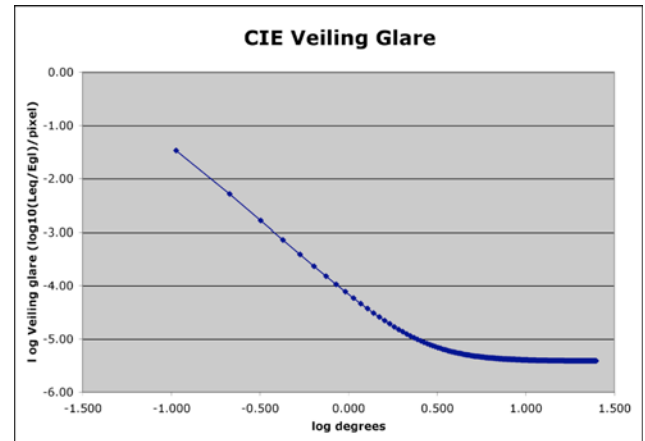


Figure 4 GSF filter plotted in log scale.

The steps for the computation are the following:

- Each pixel in the input image used to create the films used in the experiment, is converted to its optical density. Optical densities were measured from the actual films.
- The same approach is used to create the double density input values.
- All optical densities are converted into luminance.
- We create the GSF filter according to the input image size and its viewing distance (input image is padded right after with zeros, null luminance).
- The *filter* represents the spread of light from the pixel. We compute the area of the *filter* along the whole *filter* size except the center pixel, namely the amount of light energy spread from the pixel onto which is centered the filter. In fact, each pixel (donor) scatters light into all the other pixels (receivers) depending upon their reciprocal distance. Then we subtract this amount from the center pixel in order to preserve the overall amount of light in the scene. *The filter* is convoluted with the images. It has the shape taken from van den Berg's equation 8.
- The output pixel value is the sum of the target luminance plus the veiling glare from all the other pixels.

Target Luminance
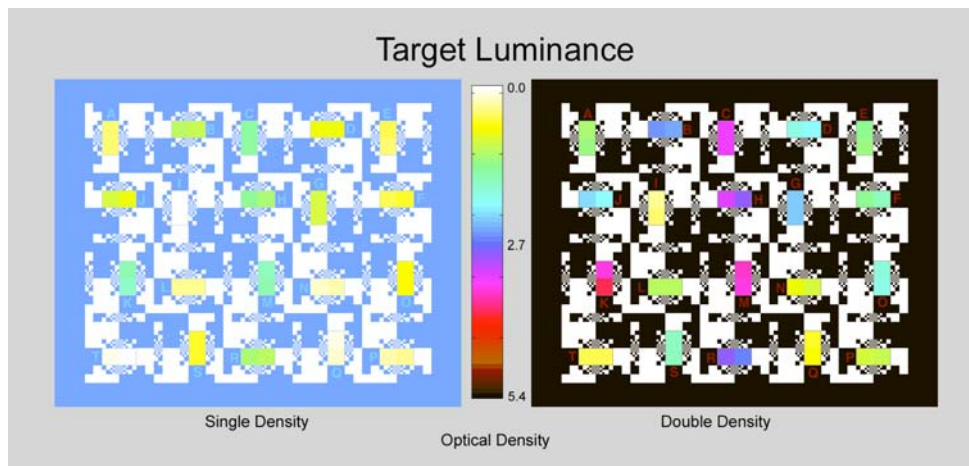
Single Density | Optical Density | Double Density

Figure 5 shows a pseudocolor rendering of target luminance. The Double-Density target has a range of 5.4 (OD); the Single Density has a 2.7 (OD) range. The colorbar in the center identifies the color of each optical density over the range of 5.4 log units. The Single- and Double-Density targets are very different stimuli.
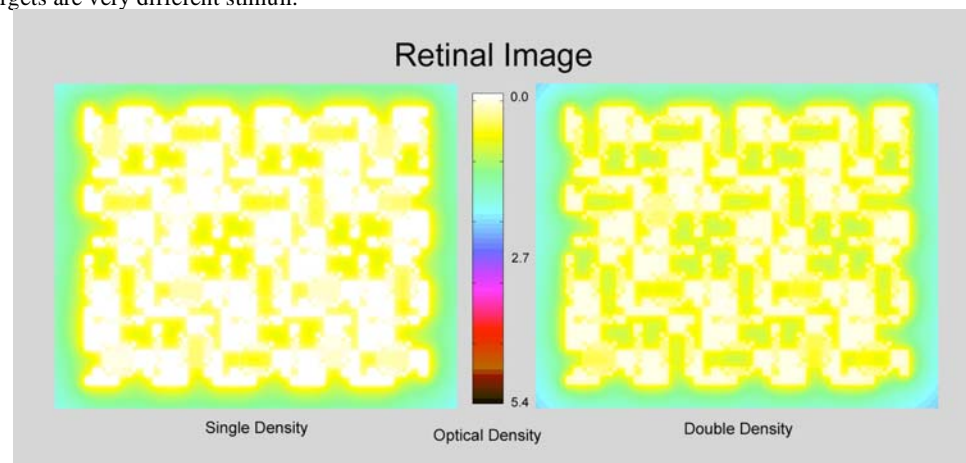


Retinal Image

Single Density | Optical Density | Double Density

Figure 6 shows the same pseudocolor rendering of retinal luminance used in Figure 5, with the same range scale. Both the Single- and Double-Density retinal ranges are less than 2.0 (OD). The Single- and Double-Density targets are very similar retinal stimuli. The Double-Density retinal image is slightly darker (bluer corners) and the Single-Density retinal image is slightly lighter



Retinal Image [OD = 0.0 to 1.0]

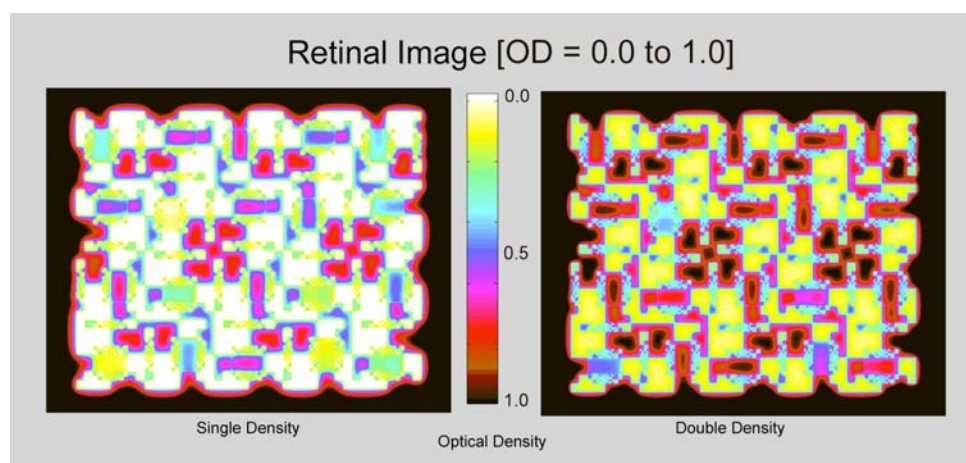Single Density | Optical Density | Double Density

Figure 7 shows a different rendition range of retinal luminance than in Figures 6, using the same colormap. To improve pseudocolor discrimination, the range of the colormap in this plot is only 1.0 (OD). This colormap rendering brings out the more subtle differences between Single- and Double-Density retinal images.

## 4.0 Analysis: Target vs. Retinal Luminance

The range of target luminances for the Single-Density target was 2.7 OD units. It is not possible to reproduce this range on print and conventional displays. The Double-Density target made the problem much more severe. We use a colormap to convert the target luminance range of 5.4 OD units to a pseudocolor rendition. We replaced the range of target luminances with 64 colors. The maximum luminance was white and the minimum was black. The colors, in decreasing luminance, are white, yellow, green cyan, blue, magenta, red brown, and black. Rendering the range of 5.4 OD target luminances in 64 steps gives a range of 0.084 OD per individual colorbar element. We show the pseudocolor scale in the center of Figure 5. The color map images illustrate the substantially different ranges of luminance measured in the 2.7 OD Single-Density and 5.4 Double-Density targets.

We used the same colormap to render the calculated retinal luminances of the Single-Density and Double-Density images (Figure 6). Unlike the Figure 5 renditions, the retinal luminances are very similar to each other. Intraocular scatter reduces the 5.4 OD dynamic range of the Double-Density target to only 2.0 log units on the retina. It is only slightly darker than the Single-Density retinal luminance array.

The calculated retinal luminances show that intraocular glare limits the range of luminances to less than 2.0 OD units for these 50% white targets. The white surround patches have nearly the same densities in both target and retinal luminances. The black surround squares have very different densities in the targets, but because of scatter, they are nearly the same in the range of retinal luminances. The 40 gray test patches have twice the density in the Double-Density target. That means that more squares have optical densities greater than 2.0. More than half the squares are below the limit determined by scattered light. Hence the gray test squares in the Double-Density targets show more retinal similarity

Figure 7 shows a different colorbar rendering of retinal luminance from that in Figure 6. Here we spread the same 64-colorbar elements over only 1.0 OD, instead of 5.4 OD. Rendering the range of 1.0 OD target luminances in 64 steps gives a range of 0.0156 OD per individual colorbar element. This rendition shows the after-scatter values of the 20 pairs different gray patches in the target. In the Single-Density target we see a range of different colors for the different transmissions. In the Double-Density target we see that intraocular scatter made many of the darker gray squares more similar.

## 5.0 Discussion

Veiling glare from a single pixel decreases with distance away from that pixel. Figure 4 shows the falloff of scattered luminance vs. distance. The value of glare reaches an asymptote with large distances. This asymptotic value is very small, but this small contribution comes from the entire image. The sum of many small contributions is a significant number. The greater the percentage of white in the scene, the more the amount of glare, the lower the contrast of the retinal image.

The background in these images has a range of different sizes of uniform white or black squares. Each white pixel scatters a fraction of its light into surrounding pixels. In turn, each pixel receives a distance-dependent fraction of light from all other pixels. A pixel in the center of a large white square has the highest retinal luminance because there are many surrounding white pixels that contribute a larger fraction of their scattered light. Similarly, the lowest luminance pixels are found in the center of the largest black square since it is the furthest from white pixel scatter sources. The highest ratio of retinal radiances (retinal contrast) is the ratio of the center pixels in largest white/black squares. The same logic shows that the smallest white/black retinal contrast is the ratio of the smallest single pixel retinal luminances. The results of the calculated retinal image show retinal luminance ratios from as high as 8.73 to 1 to as low as 1.16 to 1.

The other feature of the retinal luminance image is the conversion of uniform *target luminance* to gradients of *retinal luminance*. The target was designed to have uniform patches of white and black squares. At each white/black edge, intraocular scatter transforms the sharp edge into a gradient. The slope of that gradient varies with the neighboring pixels. The simple uniform target luminances have been transformed into a very complex array of gradients.

The final topic is the appearance of the white/black surround patches. Do they appear to have variable contrast as implied by their retinal luminance? Do they appear the same white and black for all sizes of squares? Although not measured experimentally with multiple observers and multiple trials, we observe that the white/black contrast appears essentially the same regardless of the size of the white/black squares. Intraocular scatter controls the range of retinal luminance, which in turn controls the range of usable display dynamic range. The rate of change of white/black appearance scales varies with the amount of white in the surround.[7] The mechanism responsible for simultaneous contrast makes smaller retinal luminance ratios appear more different. We have a paradox that lower retinal contrast generates higher apparent contrast.

The study of the white/black edges in the variable square surrounds suggests that apparent contrast mechanism varies with spatial-frequency channels. The calculated retinal luminance image shows that smallest squares (highest spatial-frequency components) have the smallest retinal luminance ratios.
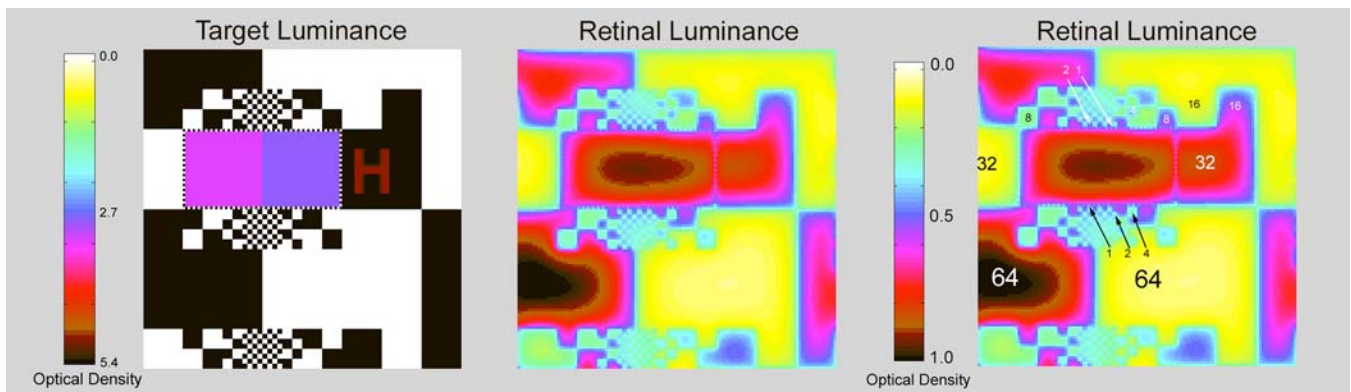
Figure 8 shows (left) the target luminance [colormap range =5.4], (center) the retinal luminance, and (right) the annotated retinal luminance using the same pseudocolor map rendition in Figures 7 [colormap range=1.0]. It shows only Double-Density Area H and its surround. It illustrates the effect of intraocular scatter on different size white and black squares.

Figure 8 illustrates the significant effects of intraocular scatter on the retinal image. It shows one of 20 different pairs of gray squares and its surround in the Double-Density target. The left panel shows the display luminances using the colorbar =5.4. The gray squares have different transmissions near 2.7 OD. All sizes of white squares have OD 0.0 and all blacks had 5.4 OD.

The retinal luminance image also shows that the largest squares (lowest spatial-frequency components) have the largest retinal luminance ratios. Nevertheless, the squares look the same whites and blacks. Regardless of the retinal luminances, the spatial processing mechanisms make the appearances the same. This suggests that different spatial frequency channels have different appearance outputs for constant retinal luminance inputs.

Figure 8 (center) shows the array of retinal luminances using colorbar=1.0. The retinal image is made of many complex gradients. The two different gray squares are now very close in retinal luminance, that they are indistinguishable in this rendering. All white squares have identical target luminances, as do all black surround squares. However, both white and black squares have variable retinal luminances depending on the size of the square. In addition, the same size square will have different retinal luminances depending on position in the surround. Constant target luminance does not ensure constant retinal luminance.

Table 2 lists the target and retinal luminances for variable size white and black surround squares in Figure 8. The locations of the square listed is shown in Figure 8 (right). The selection of these squares is arbitrary and does not represent any statistical analysis.
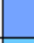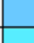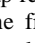
| | DD white OD | | DD black OD | | W/B contrast OD | W/B edge ratio |
|---|---|---|---|---|---|---|
| Target | 0.00 | | 5.4 | | 5.40 | 251,188.64 |
| DD 64x | 0.08 | | 1.02 | | 0.94 | 8.73 |
| DD 32x | 0.09 | | 0.89 | | 0.79 | 6.20 |
| DD 16x | 0.17 | | 0.61 | | 0.44 | 2.75 |
| DD 8x | 0.24 | | 0.43 | | 0.20 | 1.57 |
| DD 4x | 0.25 | | 0.51 | | 0.26 | 1.81 |
| DD 2x | 0.35 | | 0.47 | | 0.13 | 1.34 |
| DD 1x | 0.46 | | 0.53 | | 0.06 | 1.16 |

Table 2 lists the data and colormap rendering of white and black squares shown in Figure 8. The first column lists the areas sampled. The second and fourth columns list retinal luminance (OD). The third and fifth column show the colormap values for these densities. The sixth column lists the difference in OD. The last column lists the ratios of luminances from the center of the white and black squares. The second row shows the results for the target luminances for all squares. The remaining rows show typical samples for retinal luminance in different size squares. The third through ninth rows show sample values for the largest square (64x) through the smallest square (1x). Retinal luminance values vary considerably with the surrounding portion of the image. These are typical values identified in Figure 8. The size of white and black squares has considerable influence on the retinal luminance, contrast and white/black (W/B) ratios.

Table 2 shows the relative optical densities of retinal luminances for different size white/black pairs. It shows the colorbar rendering of these luminances. It lists the difference in OD, and the ratio of retinal luminances at the centers of the square.

Target
Luminance
5.4 OD

255.0

0.0

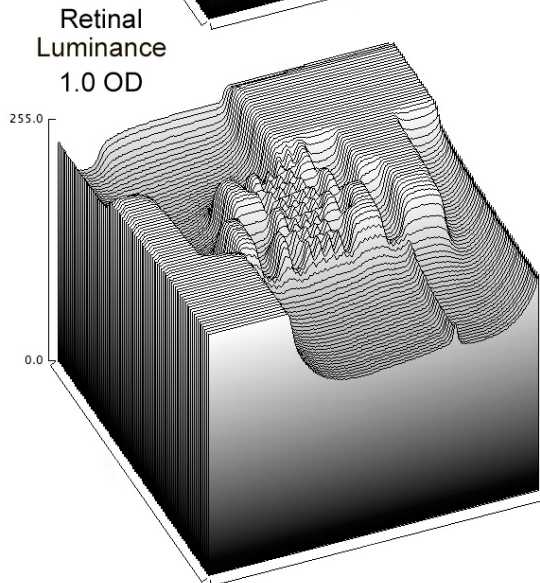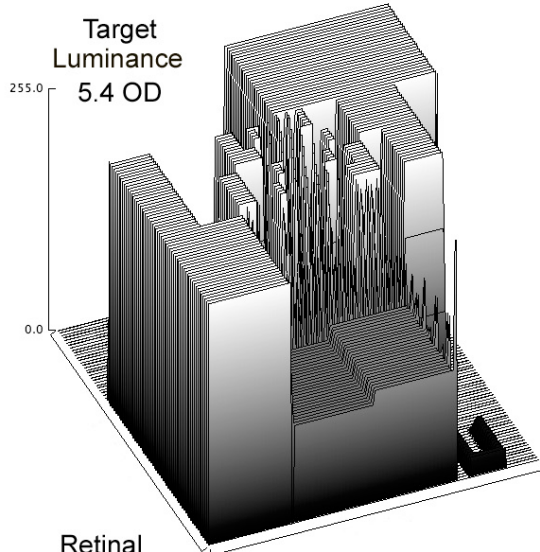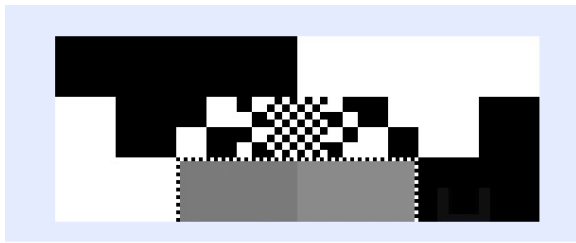Retinal
Luminance
1.0 OD

255.0

0.0

Figure 9 (top) shows the portion of the Area H target displayed as a surface plot. The bottom of the selection runs through the vertical mid-points of the two gray squares. The top, left and right limits are the ends of Area H in the target. The bottom of the area is 512 pixels wide; the height of the area is 196 pixels high.

Figure 9 (middle) show the surface plot of the target luminances. The vertical axis covers 5.4 OD units. The selected potion of the target contains 6 of 7 sizes of white and black squares. The largest three sizes are plotted correctly. The surface plot program has misrepresented the three smallest surround elements. All of the white squares should have the same values of 255. The resolution of the surface plot program limits these

high frequency square wave stimulus (this visualization problem will be corrected in the final version).

Figure 9 (bottom) shows the surface plot of the retinal luminances. The vertical axis covers 1.0 OD units. The white areas each have a different luminance value at their center depending on their size. The values of the blacks depend on their size, and their proximity to whites. The different gray values are now indistinguishable from each other. Sharp edges are replaced with complex gradients.

Figure 9 uses spatial surface map to compare the target and retinal luminances.

Intraocular scatter transforms high-dynamic-range, uniform, constant square targets into low-dynamic-range gradients with variable retinal luminance. Human spatial image processing makes this complex retinal image appear as a set of white and black squares all with the same appearance whites and blacks. HDR Image processing techniques that attempt to mimic human vision need to differentiate the optical effects of intraocular glare from neural spatial image processing. Both optical and neural mechanisms show scene-dependent alteration of the image. These different image-dependent processes tend to cancel each other, making their presence less obvious.

## Conclusions

Given the measured target luminance array, we calculated the retina luminance array using the CIE standard glare spread function. Intraocular glare reduced the high dynamic range of target luminances to much smaller ranges depending on image content. Further, the calculations show that there is no simple relationship between the retinal luminance of a pixel and its appearance between white and black. Observers report that appearance correlates better with target luminance than with retinal luminance. Complex spatial processing is required to be able to predict appearance from retinal luminance arrays.

## Additional Experiments

The proposed talk will include calculations of both 100% and 0% white surrounds. The appearance of the gray squares vs. retinal luminance will be expanded in the talk. The paper will include a detailed discussion of scatter calculations, and it will provide useful information on how to calculate retinal luminances.

# References

[1] E. Reinhard, G. Ward, S. Pattanaik, P. Debevec, *High Dynamic Range Imaging Acquisition, Display and Image-Based Lighting*, Elsevier, Morgan Kaufmann, Amsterdam, chap 6, 2006.

[2] McCann, J.J. and Rizzi, A. "Camera and visual veiling glare in HDR images", J. Soc. Information Display, vol. 15(9), 721-730 (2007).

[3] Vos, J.J. and van den Berg, T.J.T.P [CIE Research note 135/1, "Disability Glare"] ISBN 3 900 734 97 6 (1999).

[4] CIE, "146 CIE equations for disability glare", in 146/147: CIE Collection on Glare, 2002

[5] T.J.T.P. van den Berg, "Analysis ogf Intraocular Straylight, Especially in Relation to Age", *Optometry and Vision Science*, Vol. 72, No 2, pp. 52-59, 1995

[6] J. J. McCann, "Aperture and Object Mode Appearances in Images", in Human Vision and Electronic Imaging XII, eds. B. Rogowitz, T. Pappas, S. Daly, Proc. SPIE, Bellingham, WA, **6292-26**, 2007.

[7] A. Rizzi, M. Pezzetti, J.J. McCann, "Glare-limited Appearances in HDR Images", Color Imaging Conference 2007, Albuquerque (New Mexico), November 5-9, 2007.

[8] J. J. McCann and A. Rizzi, "The Spatial Properties of Contrast', in Proc. IS&T/SID Color Imaging Conference, Scottsdale; **11**, p. 51-58, 2003.

[9] Tolhurst DJ, Tadmor Y, Chao T: Amplitude spectra of natural images. Ophthalm Physiol Opt1992, 12:229-232.